Leak and Scattering Assessment by Optically Stimulated Luminescence Dosimetry in a Helical Linear Accelerator

Valoración de Fuga y Dispersión por medio de Dosimetría de Luminiscencia Estimulada Ópticamente (OSL) en un Acelerador Lineal Helicoidal

Wilson Alejandro López[1], Límbano Iván López Coello[2] , Luis Carlos Mora Garzón[3],
César Arturo Díaz Pérez[3] & Eleni Mitsoura[1]

ABSTRACT: Radiation absorbed doses to organs outside the radiation therapy treatment beam can be significant and therefore of clinical interest. Two sets of out-of-beam measurements were performed measuring the leak dose and the scattered dose, at 5 points within the accelerator components (accelerator tube and collimator) and at 21 points on the equipment and surroundings based on a positioning scheme. For this purpose, 52 Optically Stimulated Luminescence (OSL) dosimeters were used in a latest generation helical linear accelerator. Of the 200 cGy fired at a cheese-like phantom, 0.332% of the out-of-beam dose contribution was found to come from the leak and 0.784% was transformed into scattering. For these dose values, estimates of the risk of second tumors in long-term survivors indicate a reduced probability of acquiring a second secondary radiation malignancy, based on information from the 1990 BEIR Committee report.

KEY WORDS: Leak dose, scattered dose, optically stimulated luminescence, helical linear accelerator.

INTRODUCTION

The introduction of new technologies in radiotherapy has increased the effectiveness of cancer treatment, resulting in an increase in patient survival. An unfortunate side effect of the increased survival rate of patients is that there is more time for the manifestation of secondary cancer after radiotherapy (Schneider, 2011) (Kamran, 2016) (Dasu, 2017). An important factor related to the likelihood of manifestation of secondary cancer is the dose absorbed outside the treatment beam, which is the product of the accelerator leak and the scattering of the primary beam at the accelerator target. Detailed studies on the doses outside the beam have been performed (Bordy, 2013) (Kinsara, 2016) (Krya, 2017). These increase the likelihood of future complications in normal, healthy tissue. For example, the tolerance doses for the lens to induce cataracts and for the gonads are 4-15 Gy and 4-6 Gy, respectively (Henk, 1992) (Kufe, 2003). Dörr and Herrmann show in their studies that a considerable proportion of secondary

cancers occur in regions that had received doses of less than 6 Gy in previous radiation treatments (Dörr, 2002). A particular case of a new technology in radiotherapy is spiral linear accelerators, which have an energy beam of 6MV and deliver intensity modulated radiotherapy in rotation using fan beams, similar to computed tomography (Rodrigues, 2006). For this particular type of accelerator, documents for Acceptance Testing Procedures, such as TG -148 of the American Association of Physicists in Medicine (Langen, 2010) and Report 27 of the Netherlands Commission at Radiation Dosimetry (Althof, 2017), do not mention methods for quantifying doses outside the treatment beam.

The present work aims to determine the leakage and dispersion doses measured by optical stimulation luminescence dosimetry (OSL) placed at different positions around the gantry and components of the accelerator collimator using radiochromic films.

[1] Facultad de Medicina, Universidad Autónoma del Estado de México, Toluca, México.
[2] Radioterapia, Cyberrobotics, Ciudad de México, México.
[3] Hospital de Oncología, Centro Médico Nacional Siglo XXI, Ciudad de México, México.
[4] Unidad de Radioterapia, Hospital Juárez de la Ciudad de México, México.

MATERIAL AND METHOD

The studies were performed in a Radixact® helical linear accelerator (ACCURAY, 2022) at Radiotherapy Unit of Hospital Juárez in Mexico City.

When the primary beam interacts with the treatment target, it produces a total secondary dose that is external to the treatment beam and consists of two components: the scattered dose that comes from interactions in the target body (mainly Compton effect for 6MV interactions); and the leakage dose that comes from the collimating and accelerating tube components.

OSL dosimeters or nanodots (LANDAUER, 2022), have a size of 10x10x2 mm^3 and are made of carbon doped alumina (Al2O3: C) (Kerns, 2011). After irradiation with ionizing radiation, the released electrons are trapped in energy traps created by defects in the crystal. When the material is irradiated with visible light, the trapped electrons are excited, causing the pairs to recombine and emit optical photons. The flux of optical photons is proportional to the dose (Kerns, 2011).

Two series of measurements were made that triggered the treatment plan for a cheese doll. The first set of measurements used 19 OSLs on the gan-

try, 2 OSLs and 5 OSLs on the treatment table in the collimator and tube components. In this set, the dose was fired with the jaws closed and collimator multilayer (MLC) to measure the accelerator leakage dose. In the second set to measure scatter, the OSLs were placed in the same positions as in the previous set, and the dose of the plan was fired up without any blocking using the original parameters of the treatment plan for the cheese phantom.

Treatment Planning in Helicoidal Therapy

A treatment plan was created in helical mode in the Precision® planning software . Previously, a series of tomography images of a cheesy phantom with an electronic density similar to that of water was imported; in the same way, the structures were segmented for planning. This plan was optimized with a beam width of 5 cm, a pitch of 0.5, and a modulation factor of 2 (see Figure 1).

The blank volumes used for this plan were irradiated with a dose fraction of 200 cGy in 15 sessions, corresponding to a total dose of 30 Gy.

OSL Calibration

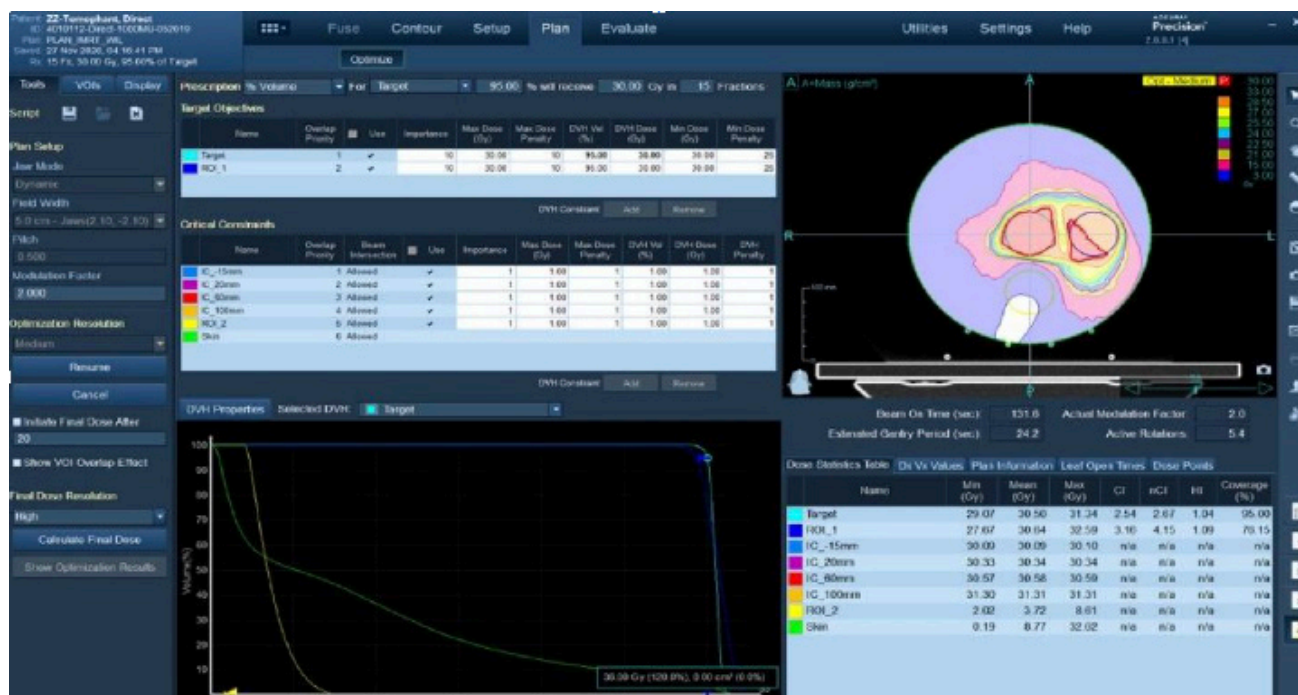The OSL dosimeters were positioned on plates of solid water of 30x30x1 cm^3 and density

Fig. 1. Tomo-phantom treatment plan, the target structures and critical structures can be seen. The target structures are prescribed 30 Gy in 15 fractions, each dose fraction is 200 cGy.

1.045 g/cm³. The plates were previously placed on the treatment table at an axis-source distance of 85 cm. Bolus 1.5 cm thick were also used to cover the OSL dosimeters to reproduce the maximum dose condition for a beam of 6 MV with a size of 5x40 cm². The OSL dosimeters were irradiated with doses of 0.5, 1, 2, 5, 7, 20, 50, 100, 200, 500, 760 and 1000 cGy (Figure 2).
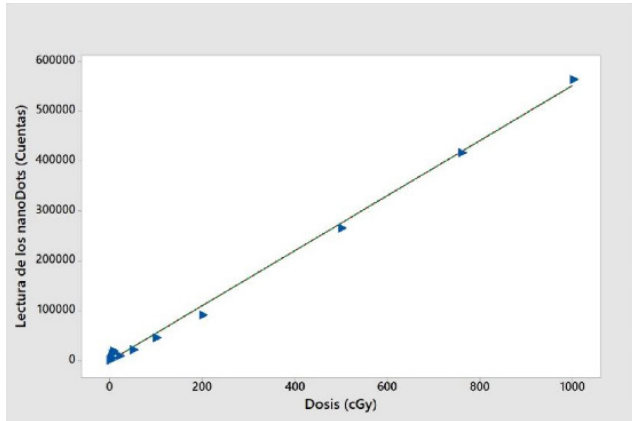

Fig. 2. OSL calibration curve, 6 MV beam.

After irradiation, the dosimeters were sent to the Microstar® reading system (LANDAUER, 2022)to obtain the reference values.

Internal positioning of OSL dosimeters

Using 20 radiochromic foils of 2x2 cm², 5 measurement points were selected according to their optical density to position the OSL in the colli-
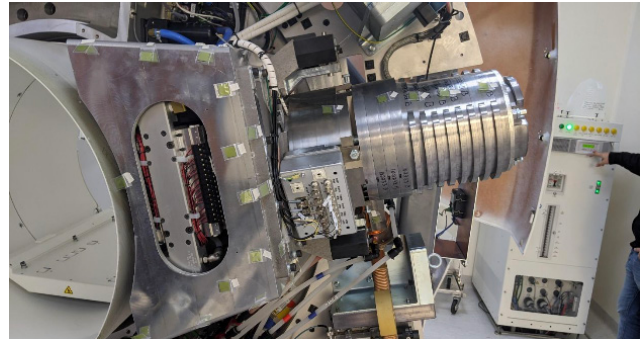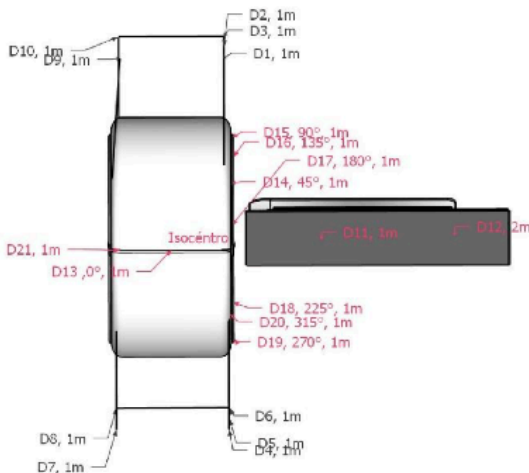

Fig. 3. Random positioning of EBT3 radiochromic foils in the tube, waveguide and collimation of Radixact: Hospital de Juárez de la Ciudad de México.

mator and accelerating tube (see Figure 3). In addition to this procedure, the Figure 4 shows a map of the positioning of the OSLs in the devices and the surrounding area was created.

The OSLs in the equipment were located one meter from the isocenter, at gantry angles of 0 °, 45 °, 90 °, 135 °, 180 °, 225 °, 270 °, and 315 °. The OSLs on the table are located one meter and two meters from the isocenter. The remaining OSLs are located one meter away from the indicated positions to determine dose levels near the bunker primary barriers. A total of 26 OSL per set were used for this work.

RESULTS

The treatment planning was shot at three revolutions per minute, and the films with the highest optical density were located from the following po-
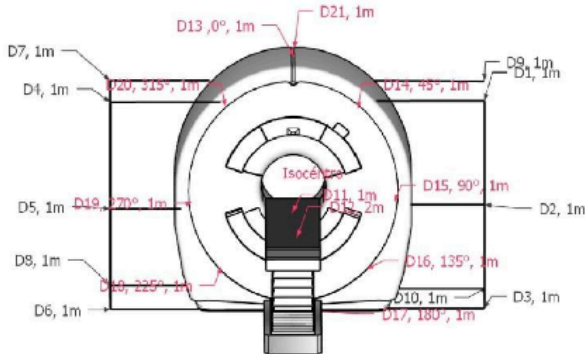

Fig. 4. Positioning of the OSL dosimeters: The diagram shows the positions of the OSL dosimeters in the plant and in the surrounding area. There are a total of 21 measurement points in this diagram. For the identification of the position, three components were used as abbreviations, D#, the angle in the portal and the distance ex. D14, 45°, 1m: "The dose at position 14 at 45° at one meter from the isocenter". Points with two components, e.g., D1, 1m: "The dose at position 1 at one meter from D14,45°, 1m".

sitions: two points near the MLC (Figure 5c), one point on the inside of the collimator cheeks in the direction of the Y axis (Figure 5a). Also, one point on the accelerator waveguide and one (1) point at the junction of the collimator with the tube (Figure 5b), for a total of five points.
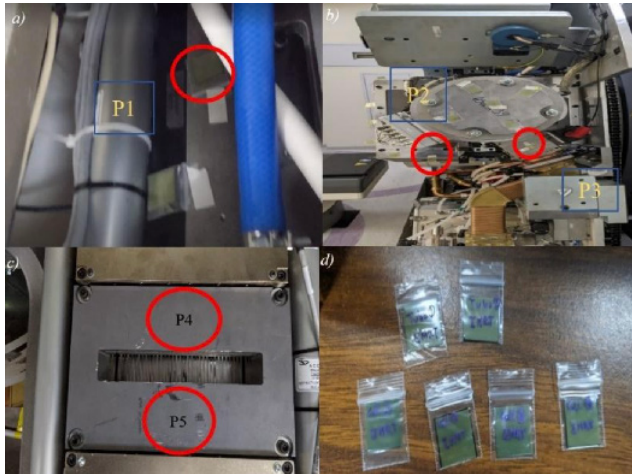

Fig. 5. In this series of images, the red circle is used to show the five positions where the radiochromic films show greater attenuation. In (a), the inside of the cheeks of the collimator can be seen. The position P1 is observed. Figure b shows the position P2 the connection of the tube with the collimator, also in this figure the waveguide P3 can be seen. Figure c shows the MLCs with positions P4 and P5. In 6d, the 6 films that were most attenuated are indicated. One film was discarded to finalize the five positions.

After determining the points of greatest attenuation within the gantry, the OSL dosimeters were placed in the same location for leakage and dispersion measurements (Figure 6).
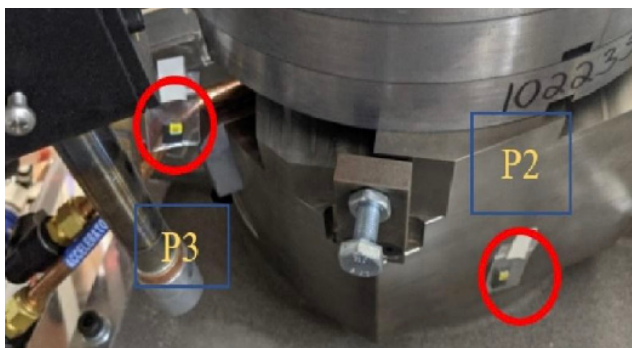

Fig. 6. Position of the OSLs on the P3 waveguide and the base of the P2 tube.

After triggering the treatment planning in the above modalities, the leakage and scattering dose data of the components are shown in Table I.

Table I: Absorbed dose of the five positions within the accelerator components

Ubication	Dose (cGy)	Dose (cGy)	Ratio (LD/SD)
Inner cheek Coll P1	1.722	4.251	0.405
Tube Base P2	1.803	4.262	0.423
Waveguide P3	3.461	6.730	0.514
MLC P4	4.175	10.390	0.402
MLC P5	4.301	11.320	0.380

Relative to all OSL located on the map and in the components, Table II summarizes values of the leakage and scattering doses measurement.

DISCUSSION

Regarding the leakage and dispersion data in the accelerator components, due to the bremsstrahlung being produced at the same level of the waveguide, it was assumed that this would be the point of highest dose in the facility, but this was not the case as the values of maximum dose contribution in this study were close to the MLC.

According to Tabla I, within the accelerating tube and collimating components in these five positions measured for leakage dose, the minimum dose was 1,722 cGy in the inner part of the collimator cheek, compared to the maximum dose where 4,301 cGy was obtained in the F5 position near the MLCs, and the average of the values in the five positions is 3.1 cGy. In contrast, for the scatter values, the minimum dose was 4,251 cGy and the maximum dose was 11,320 cGy, and the positions were invariant with respect to the leakage dose values, and the average for the five positions was 7.4 cGy.

Table II: Descriptive statistics of the leakage dose and scatter of the 26 OSL located in the accelerator and in the surrounding area.

Variable	N	Average	Mean Error	Des. Est.	Variance	Mín. Value	Máx. Value
Leakage Dose (LD)	26	0.644	0.259	1.318	1.738	0.006	4.301
Scattered Dose (SD)	26	1.568	0.626	3.192	10.189	0.026	11.32

Figure 6 shows the magnitude and behavior of the dose outside the treatment beam, in general, the leakage doses with the highest magnitude are in the 13 measurement points in the equipment with, except for one value, which is at 0 °, behind the gantry. While in the scattering, the values increase at the same points of the leakage dose, the point increases to one meter and from the treatment Table.

The maximum values for the two study components are within the collimation and acceleration tube components of the facility and the minimum values are at 0 degrees behind the device portal. It can be assumed that the secondary dose, i.e., the sum of the two average components, yields a value of 2,212 cGy of the 200 cGy administered in the treatment planning (see Table II).

Of the 200 cGy produced in the primary beam after its interaction with the target, 0.332% of the dose is the leak component and 0.784% is converted to the dispersion, since it is logical to have a larger amount of dose in the dispersion.

Despite considerable uncertainty, it is of interest to assess the risk to patients from the out-of-treatment dose and the potential benefit of lowering that dose.

The long-term risk of a second neoplasm can be estimated from data published in the BEIR Committee Report (Council, 1990). If a 30-year-old man receives 1 Gy to one of his lungs, the estimated additional risk of developing lung cancer within his life expectancy of 40.5 years would be about 1%

(That is, the risk of cancer would be 1% higher than the risk if this dose of radiation had not been received.) This value was determined using an excess risk for lung cancer of 3×10^{-4} Gy^{-1} y^{-1} and 30.5 years of risk. Similarly, a 30-year-old woman receiving 1 Gy in one breast would have a 3% increased risk of developing breast cancer within her life expectancy of 47 years. This value was determined using an absolute excess risk for breast cancer of 8.7×10^{-4} Gy^{-1} y^{-1} and 37 years of risk time (Council, 1990). For almost all other organs, the estimated excess risk is about 1%.

For 200 cGy with a beam of 6 MV, the average doses outside the device at one meter for leakage and scatter are respectively: 0.0306 cGy and 0.0732 cGy. If 60 Gy are fired at the end of a treatment, this results in 0.918 cGy per leak and 2.196 cGy per scatter. These doses are less than 1 Gy, so the probability of a second cancer in the lung for a 40.5-year-old male would be 0.031% and for a 30-year-old female the risk of a second cancer at 47 years would be 0.093%.

CONCLUSION

The average value of the leakage and scatter dose of the 26 measured points for 200 cGy for the helical technique was (0.644 ± 0.259) cGy and (1.568 ± 0.626) cGy, respectively.

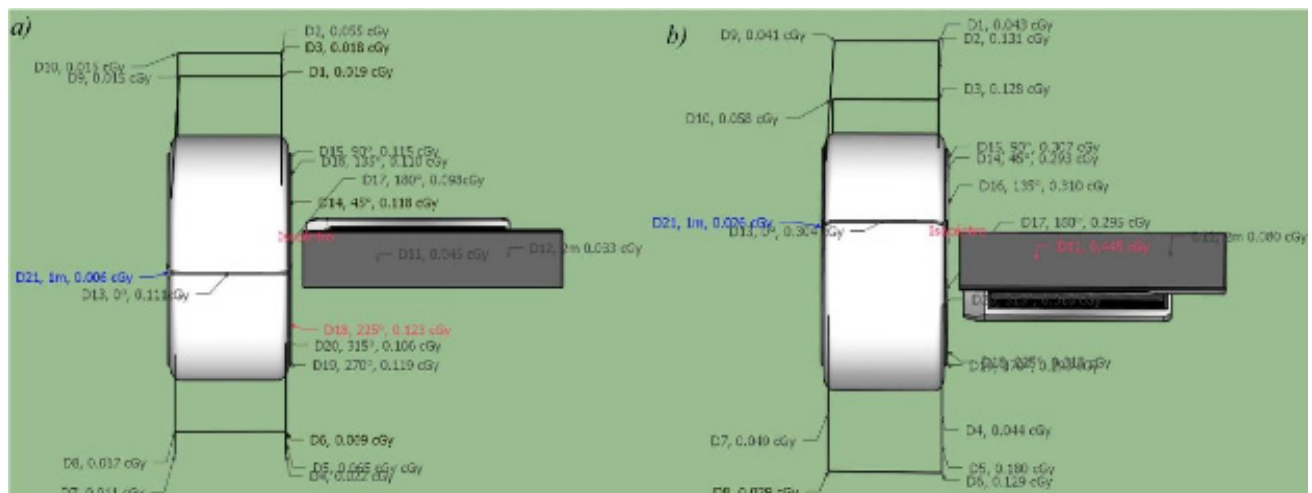The values obtained for the components of the out-of-beam dose show a significantly reduced

Fig. 7. In 7a, the results of the leakage dose. In 7b the results of the dose by dispersion. The red position is the maximum dose in the OSLs located on the facility and the blue position is the minimum dose in the accelerator.

probability of secondary cancer compared to the estimates of excess risk published by the BEIR-V Committee. This confirms that the delivery system is designed to maximize shielding against radiation leakage.

Acknowledgment

RESUMEN: La dosis absorbida de radiación a órganos fuera del haz de tratamiento de radioterapia puede ser significativa y, por lo tanto, de interés clínico. Se realizaron dos sets de mediciones fuera del haz para determinar la dosis de fuga y la dosis dispersa, en 5 puntos dentro de los componentes del acelerador (tubo de aceleración y colimador) y 21 puntos en el equipo y alrededores basado en un esquema de posicionamiento. Para este fin se utilizaron 52 dosímetros de luminiscencia estimulada ópticamente (OSL, Optically Stimulated Luminescence), en un acelerador lineal helicoidal de última generación. De los 200 cGy disparados a un maniquí tipo queso, se encontró que el 0.332% de la contribución de dosis fuera del haz provenía de la fuga y 0.784% se transforma en dispersión. Para estos valores de dosis, las estimaciones del riesgo de segundos tumores en los supervivientes a largo plazo indican una reducida probabilidad de contraer una segunda malignidad por radiación secundaria, según la información del informe del Comité BEIR de 1990.

PALABRAS CLAVES: Dosis de fuga, dosis dispersa, dosímetros de luminiscencia estimulada ópticamente, acelerador lineal helicoidal.

REFERENCIAS BIBLIOGRÁFICAS

ACCURAY, I., 2022. RADIXACT. (Online) Available at: https://www.accuray.com/radixact/ (Accessed 24 02 2022).

Althof, V., 2017. Quality Assurance for Tomotherapy Systems, Amsterdam: Netherlands Commission on Radiation Dosimetry.

Bordy, J., 2013. Radiotherapy out-of-field dosimetry: Experimental and computational results for photons in a water tank. Radiation Measurements, pp. 29-34.

Council, N. R., 1990. Health Effects of of Exposure to Low Levels of Ionizing Radiation of Ionizing Radiation: BEIR, Washington: The National Academies Press.

Dasu, A., 2017. Models for the risk of secondary cancers from radiation therapy. European Journal of Medical Physics, pp. 2-7.

Dörr, W., 2002. Second primary tumors after radiotherapy for malignancies treatment-related parameters.. Strahlentherapie und Onkologie, pp. 357-362.

Henk, J., 1992. Radiation dose to the lens and cataract formation, London: International Journal of Radiation Oncology, Biology and Physics.

Kamran, S. C., 2016. Therapeutic Radiation and the Potential Risk of Second. Wiley Online Library, pp. 1809-1821.

Kerns, J. R., 2011. Angular dependence of the nanoDot OSL dosimeter. American Association of Physicists in Medicine, 38(7), pp. 3955- 3962.

Kinsara, A., 2016. Review of Leakage from a Linear Accelerator and Its Side Effects on Cancer Patients. Journal of Nuclear Medicine & Radiation Therapy, pp. 7-6.

Krya, S. F., 2017. Measurement and calculation of doses outside the treated volume from external-beam radiation therapy. The International Journal of Medical Physics Research and Practice, pp. e391-e429.

Kufe, D., 2003. Holland-Frei Cancer Medicine. New York: BC Decker.

LANDAUER, 2022. MICROSTAR. (Online) Available at: https://www.landauer.com/microstarii (Accessed 24 02 2022).

LANDAUER, 2022. NANODOTS. (Online) Available at: https://www.landauer.com/product/nanodot (Accessed 24 02 2022).

Langen, K., 2010. QA for helical tomotherapy: Report of the AAPM Task Group 148. American Association of Physicists in Medicine, pp. 4817-4853.

Rodrigues, G., 2006. A comparison of prostate IMRT and helical tomotherapy class solutions. The green journal, p. 374–377.

Schneider, U., 2011. Modeling the Risk of Secondary Malignancies after Radiotherapy. Genes, pp. 1033-1049.

Dirección para correspondencia:
Wilson Alejandro López
Facultad de Medicina
Universidad Autónoma del Estado de México

Toluca
MÉXICO